THE JOURNAL OF BIOLOGICAL CHEMISTRY VOL. 288, NO. 38, pp. 27358–27365, September 20, 2013

Control by Potassium of the Size Distribution of *Escherichia coli* FtsZ Polymers Is Independent of GTPase Activity*

Received for publication, May 3, 2013, and in revised form, July 26, 2013 Published, JBC Papers in Press, August 12, 2013, DOI 10.1074/jbc.M113.482943

Rubén Ahijado-Guzmán[‡], Carlos Alfonso[‡], Belén Reija[§], Estefanía Salvarelli[¶‖], Jesús Mingorance[¶], Silvia Zorrilla[§1], Begoña Monterroso[‡2], and Germán Rivas[‡3]

From the [‡]Centro de Investigaciones Biológicas, Consejo Superior de Investigaciones Científicas (CSIC), 28040 Madrid, the [§]Instituto de Química-Física Rocasolano, CSIC, 28006 Madrid, the [¶]Servicio de Microbiología, Hospital Universitario La Paz, IdiPAZ, 28046 Madrid, and [‖]Biomol Informatics SL, Cantoblanco, 28049 Madrid, Spain

Background: GTP-linked FtsZ assembly/disassembly is central for bacterial division.
Results: The size of the narrowly distributed GTP-FtsZ polymers decreases upon lowering potassium and is independent of GTPase activity.
Conclusion: Potassium oppositely controls the size distribution of GTP-FtsZ polymers and the abundance of GDP oligomers.
Significance: The narrow size distribution is a particularity of FtsZ polymers maintained under a variety of solutions conditions, with potential biological implications.

The influence of potassium content (at neutral pH and millimolar Mg^{2+}) on the size distribution of FtsZ polymers formed in the presence of constantly replenished GTP under steady-state conditions was studied by a combination of biophysical methods. The size of the GTP-FtsZ polymers decreased with lower potassium concentration, in contrast with the increase in the mass of the GDP-FtsZ oligomers, whereas no effect was observed on FtsZ GTPase activity and critical concentration of polymerization. Remarkably, the concerted formation of a narrow size distribution of GTP-FtsZ polymers previously observed at high salt concentration was maintained in all KCl concentrations tested. Polymers induced with guanosine 5′-(α,β-methylene)triphosphate, a slowly hydrolyzable analog of GTP, became larger and polydisperse as the potassium concentration was decreased. Our results suggest that the potassium dependence of the GTP-FtsZ polymer size may be related to changes in the subunit turnover rate that are independent of the GTP hydrolysis rate. The formation of a narrow size distribution of FtsZ polymers under very different solution conditions indicates that it is an inherent feature of FtsZ, not observed in other filament-forming proteins, with potential implications in the structural organization of the functional Z-ring.

FtsZ is a key component of the bacterial cell division machinery (1) that is able to form polymers whose GTP-dependent assembly/disassembly is crucial for the formation of the dynamic division ring (1, 2). *Escherichia coli* FtsZ has been shown to polymerize in dilute physiological buffers at neutral pH and millimolar magnesium concentration into one-subunit-thick protofilaments (1). In addition to pH (3, 4), nucleotides and secondary (5, 6) and primary (7) cations have also been shown to determine FtsZ polymerization. Monovalent cations have been found to be responsible for the dynamic behavior of the polymers (7), and it has been proposed that K^+ concentration affects both the GTPase activity and morphology of GTP-FtsZ polymers (8). K^+ binding is indispensable for polymerization of *E. coli* FtsZ at physiological pH, and although assembly can also be triggered by other monovalent cations, it is unlikely that they play a physiological role given their low affinity for FtsZ (7).

Our laboratory has studied the assembly of FtsZ in the presence of GTP and guanosine 5′-(α,β-methylene)triphosphate (GMPCPP)[4] (5, 9), a slowly hydrolyzable analog of GTP, at 500 mM KCl and neutral pH. The protofilaments formed in the presence of GTP are very dynamic, rapidly disassembling with nucleotide depletion due to hydrolysis. By adding an enzymatic GTP regeneration system (10), the polymers are maintained at steady state for the time period required to be analyzed by biophysical methods (5, 9). In contrast, GMPCPP triggers self-assembly of FtsZ into polymers that are stable for longer times (2), allowing the study of the influence of the polymer cofactors under slow hydrolysis conditions and, therefore, the influence of hydrolysis in polymer remodeling. We found that, in the presence of either of these nucleotides, as the concentration of protein increases, FtsZ undergoes a concerted transition between a paucidisperse distribution of low molecular weight species and a narrow size distribution of high molecular weight species containing on the order of 100 (GTP-FtsZ) or ~160 (GMPCPP-FtsZ) monomers (5), in good agreement with independent atomic force microscopy data (11). The peak size of

* This work was supported in part by Human Frontier Science Program Grant RGP0050/2010; European Commission Contract HEALTH-F3-2009-223431 (to G. R.); and Spanish Government Grants BIO2008-04478-C03 (to G. R.), CSIC PIE-201020I001 (to C. A.), BFU2010-14910 (to S. Z.), and BIO2011-28941-C03 (to G. R. and S. Z.).
[1] Present address: Centro de Investigaciones Biológicas, CSIC, 28040 Madrid, Spain.
[2] To whom correspondence may be addressed: Centro de Investigaciones Biológicas, CSIC, Ramiro de Maeztu, 9, 28040 Madrid, Spain. Tel.: 34-91-837-3112; Fax: 34-91-536-0432; E-mail: monterroso@cib.csic.es.
[3] To whom correspondence may be addressed: Centro de Investigaciones Biológicas, CSIC, Ramiro de Maeztu, 9, 28040 Madrid, Spain. Tel.: 34-91-837-3112; Fax: 34-91-536-0432; E-mail: grivas@cib.csic.es.

[4] The abbreviations used are: GMPCPP, guanosine 5′-(α,β-methylene)-triphosphate; SV, sedimentation velocity; FCS, fluorescence correlation spectroscopy; DLS, dynamic light scattering.

this distribution varies with nucleotide type and, in the case of GTP-FtsZ polymers, also with the concentration of Mg^{2+}, but the concerted nature of the transition does not. A further increase in protein concentration increases the population of high molecular weight species but not the mean size or dispersity, suggesting a second-order phase transition. Since our initially published results (9), we have accumulated additional data by a variety of techniques that not only corroborate and strengthen our initial observations but provide further additional information regarding the dependence of FtsZ polymerization on its cofactors.

Here, we present a comprehensive study of the KCl dependence of the size and homogeneity of GTP-FtsZ polymers using a combination of biophysical methodologies. We also studied the effect on GMPCPP-FtsZ polymers, and the differences between both types of polymers are emphasized. We compared the behavior of GTP-FtsZ polymers regarding their modulation by KCl with that previously reported for GDP-FtsZ (12), and additional new data are discussed. The results presented here may also help to clarify some of the discrepant conclusions regarding FtsZ polymerization drawn by several laboratories on the basis of experiments conducted under different solution conditions.

EXPERIMENTAL PROCEDURES

Protein Purification, Labeling, and GTPase Activity—FtsZ was purified and labeled with Alexa Fluor 488 as described (12, 13). Experiments were performed in working buffer (50 mM Tris-HCl (pH 7.5) and 5 mM Mg^{2+} unless stated otherwise) supplemented with the specified concentrations of KCl. GTP-FtsZ polymers were stabilized by an enzymatic GTP regeneration system (15 mM acetyl phosphate and 2 units/ml acetate kinase) (14), except for anisotropy measurements. GTPase activity was measured by the Malachite green method as described (15). Briefly, 10 μM FtsZ in working buffer supplemented with the required KCl concentration was incubated at 22 °C with 1 mM GTP or GMPCPP. Samples were collected at different times and diluted in buffer containing 65 mM EDTA to stop the reaction. Malachite green-molybdate reagent was added, and absorbance was measured at 620 nm. Phosphate concentrations were calculated from a Na_2HPO_4 standard curve, and the velocity values of the GTPase activity (V) were determined in nmol of phosphorus/nmol of FtsZ/min from the slope of the linear part of the phosphate accumulation curves. The data presented correspond to the mean ± S.D. of at least three experiments.

Sedimentation Velocity (SV)—Experiments were conducted in a Beckman Optima XL-I ultracentrifuge (Beckman Coulter) as described (5). Sedimentation coefficient distributions were calculated with SEDFIT (16). Sedimentation values were corrected to standard conditions (water, 20 °C, and infinite dilution) to obtain $s_{20,w}$ using SEDNTERP (17). The continuous molar mass distributions ($c(M)$) were calculated as described (16). Frictional ratios (f/f_0) were independently determined from the sedimentation and diffusion coefficients as described (5).

Composition Gradient Static Light Scattering—Monitoring the concentration dependence of FtsZ scattering at 90° in a modified miniDAWN light scattering photometer (Wyatt Technology Corp., Santa Barbara, CA) and data analysis were conducted as described (18). Because of the angular dependence of the scattering of FtsZ polymers (5), the scaled Rayleigh ratio (R/K_o) is not a direct measurement of the molar mass but is proportional, and it is here shown for comparison of the properties of different species depending on the solution composition.

Fluorescence Correlation Spectroscopy (FCS)—FCS measurements were carried out on a MicroTime 200 instrument (PicoQuant GmbH) with two-photon excitation as described (5, 13). Data analysis was conducted by fitting a three-component model involving a fast species corresponding to free dye and two other species corresponding to unassembled and assembled FtsZ. The contribution of the free dye (10–20%) and its diffusion were independently measured and fixed in the analysis. The translational diffusion of unassembled FtsZ was likewise independently measured and fixed in the analysis of GTP- or GMPCPP-FtsZ, keeping its contribution together with the parameters defining the polymer as adjustable values, as described in detail elsewhere (5).

Steady-state Fluorescence Anisotropy—Anisotropy measurements to determine the FtsZ critical concentration of polymerization at 100 mM KCl were performed using a PC1 photon counting steady-state spectrofluorometer (ISS) and analyzed as described previously (13). Measurements were conducted at 20 °C with excitation and emission wavelengths of 481 and 520 nm, respectively, and with 0.15 μM Alexa Fluor 488-labeled FtsZ.

Dynamic Light Scattering (DLS)—DLS experiments were conducted in a Protein Solutions DynaPro MS/X instrument as described (5). Data were collected and exported with Dynamics V6 software and analyzed using user-written scripts and functions in MATLAB (Version 7.10, MathWorks, Natick, MA). The obtained autocorrelation functions were analyzed as described (5) to get the apparent diffusion coefficient.

Estimate of Molar Mass from Hydrodynamic Measurements—The apparent molar mass of FtsZ polymers was calculated via the Svedberg equation (19) using the average $s_{20,w}$ obtained from analysis of independent SV profiles and the average of the standard D values obtained by DLS and FCS as described (5, 20).

Electron Microscopy—EM samples and imaging were done as described (8). Briefly, FtsZ was incubated with the nucleotide for 1 min, added to a carbon-coated glow-discharged copper grid, stained with uranyl acetate, and visualized under a JEOL JEM-1230 microscope at 100 kV.

RESULTS

Lowering the KCl Concentration Reduces the Size of GTP-FtsZ Polymers—SV experiments on FtsZ polymers showed that, at 500 mM KCl, a 13–14 S species was the main sedimenting material (Fig. 1), in agreement with our previous results (5, 9). Upon lowering the KCl concentration, the sedimentation coefficient distributions were still well described by a major peak of fast sedimenting species, but s values changed at 300 and 100 mM KCl. The profiles in Fig. 1 are shown as representative of typical data. Interestingly, the KCl-driven variation in the s value proved to be reversible, as the sedimentation profile of

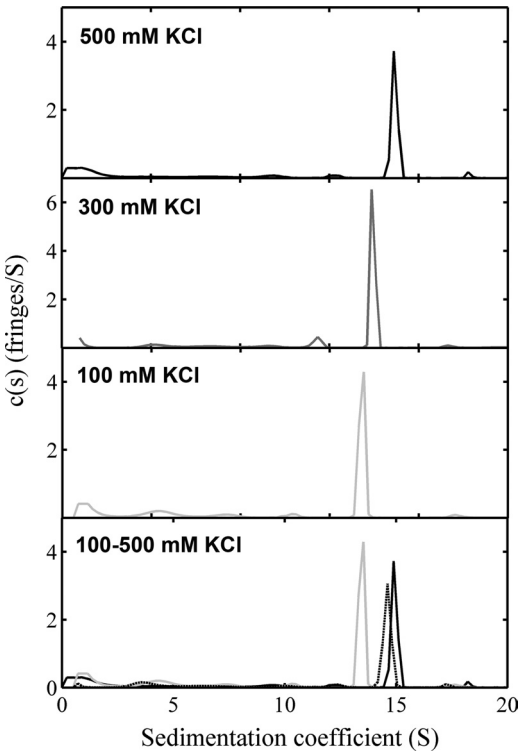

FIGURE 1. **Effect of KCl on GTP-FtsZ sedimentation.** Shown are typical sedimentation coefficient distributions of FtsZ (12 μM) with 1 mM GTP and an enzymatic GTP regeneration system in working buffer with the specified KCl concentrations. The *lower panel* shows FtsZ polymerized in 100 mM KCl and, after a 5-min incubation, supplemented with concentrated KCl to reach a final concentration of 500 mM (*dotted line*). Sedimentation profiles of FtsZ polymerized in 500 mM KCl (*black line*) or 100 mM KCl (*gray line*) are included as reference.

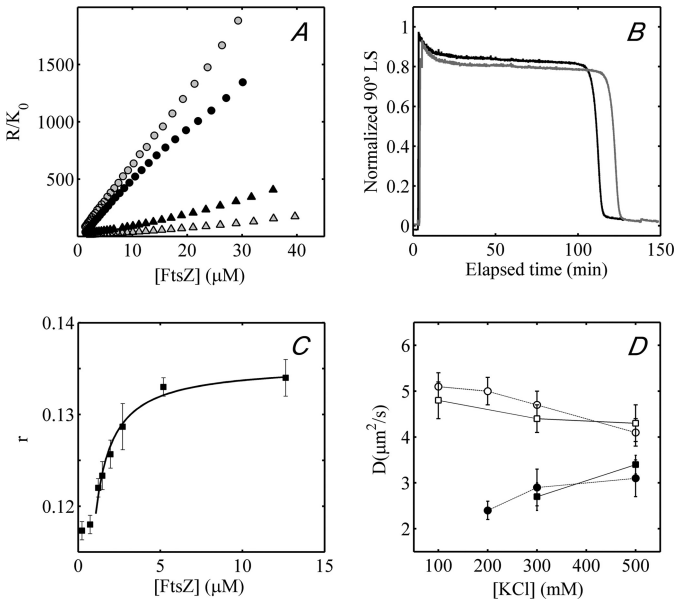

FIGURE 2. **Effect of KCl on GTP-FtsZ assembly.** *A*, concentration dependence of 90° scattering of FtsZ at 500 KCl (*gray symbols*) and 100 mM KCl (*black symbols*) with GTP (*circles*) and GDP (*triangles*). *B*, time-dependent scattering of GTP-FtsZ polymers in working buffer supplemented with 500 mM KCl (*black line*) or 100 mM KCl (*gray line*). *LS*, light scattering. *C*, dependence of fluorescence anisotropy of Alexa Fluor 488-labeled FtsZ with total FtsZ concentration in working buffer with 100 mM KCl. The concentration of Alexa Fluor 488-labeled FtsZ was 0.15 μM, and additional unlabeled FtsZ was added up to the final concentration. The *solid line* is the best fit of the model described in Ref. 13. The isotherm is the mean ± S.D. of three independent experiments. *D*, dependence of $D_{20,w}$ of GTP-FtsZ (*white symbols*) and GMPCPP-FtsZ (*black symbols*) on KCl concentration as determined by FCS (*circles*) and DLS (*squares*). Data are the mean ± S.D. of at least three independent experiments. the FtsZ concentration was 12 μM.

GTP-FtsZ polymers formed in 100 mM KCl and subsequently supplemented to 500 mM was practically the same as that of polymers formed at the higher salt concentration (Fig. 1). Independent composition gradient static light scattering and translational diffusion measurements (see below) allowed us to conclude that the observed decrease in the *s* value was in fact due to a reduction in the size of FtsZ polymers.

The intensity of the 90° scattering of FtsZ polymers decreased, within the same protein concentration range, as the KCl concentration was lowered (Fig. 2*A*), indicating a reduction in the polymer size. It is noteworthy that parallel experiments on FtsZ-GDP at equivalent protein concentrations showed the opposite trend, *i.e.* the size of the FtsZ oligomers increased upon lowering the salt content (Fig. 2*A*), in good agreement with previously published analytical ultracentrifugation results (12). Time-dependent scattering measurements allowed us to discard depletion of nucleotide due to inefficient GTP regeneration at KCl concentrations below 500 mM as a factor determining the smaller size of the polymers, as at both extremes of the KCl concentration range tested, they were stable throughout the time course of all the experiments conducted (Fig. 2*B*). Composition gradient static light scattering experiments ruled out a major effect of KCl concentration on the critical concentration of polymerization of FtsZ, as further confirmed by fluorescence anisotropy measurements (Fig. 2*C*), rendering values of 1.04 ± 0.07 μM (0.042 ± 0.003 g/liter) at 100 mM KCl, only slightly smaller than that at 500 mM KCl, ~1.24 μM (~0.05 g/liter) (9, 13).

The decrease in mass of the FtsZ filaments at lower KCl concentrations was further confirmed by their faster diffusion (Fig. 2*D* and Table 1) as measured by FCS and DLS, which, together with the slower sedimentation, constitute a clear indication of mass decrease. Although the error intervals may overlap in some cases when average data arising from different experiments were compared (Table 1), it is worth mentioning that, within a single experiment performed at different KCl concentrations on the same day and with the same samples, the same trend was always observed, higher *s* and lower *D* values with increasing KCl concentration. Estimated interval values of monomers per polymer for a given salt concentration in Table 1 were calculated considering the variability found in the *s* values within protein preparations, reduced with 500 mM KCl. The apparent mass for GTP-FtsZ in 100 mM KCl calculated via the Svedberg equation corresponds to protofilaments of ~40–70 monomers, in reasonable agreement with EM determinations under similar experimental conditions (8). This value is lower than the Svedberg estimation for FtsZ protofilaments at 500 mM KCl (Table 1). EM images of GTP-FtsZ polymers under our experimental conditions also show a decrease in the average size of the fibrils at 100 mM KCl (Fig. 3*A*) compared with those at 500 mM KCl (see supplemental Fig. S2 in Ref. 21).

The apparent mass of the polymers was also estimated from *c*(*M*) analysis of SV profiles at each salt concentration. The

TABLE 1

Dependence of biophysical properties of GTP- and GMPCPP-FtsZ polymers on KCl content

Measurements were performed using 12 μM FtsZ in working buffer.

[KCl]	$s_{20,w}$ [a]	D_{20} DLS	D_{20} FCS	n [b]	f/f_0 [c]	n [d]
	S	$\mu m^2/s$	$\mu m^2/s$			
GTP						
500 mM	15.1 ± 1.7	4.3 ± 0.4	4.1 ± 0.3	70–100	5.1	70–90
300 mM	13.9 ± 2.0	4.4 ± 0.3	4.7 ± 0.3	60–80	5.0	60–80
200 mM			5.0 ± 0.3			
100 mM	11.9 ± 2.5	4.8 ± 0.4	5.1 ± 0.3	40–70	5.0	40–70
GMPCPP						
500 mM	19.9 ± 0.1	3.4 ± 0.2	3.1 ± 0.4	140–180	5.9	140–170
300 mM	29.6 ± 0.1	2.7 ± 0.3	2.9 ± 0.4	220–310	6.0	170–300
200 mM			2.4 ± 0.2			
100 mM	>38					

[a] Major species when several are present.
[b] Monomers per polymer, calculated from apparent molar mass via the Svedberg equation from the sedimentation coefficient interval and the average *D* values by DLS and FCS.
[c] Frictional ratio, calculated from the $s_{20,w}$ interval and the average of $D_{20,w}$ by DLS and FCS.
[d] Monomers per polymer, calculated from $c(s)$ distributions and f/f_0.

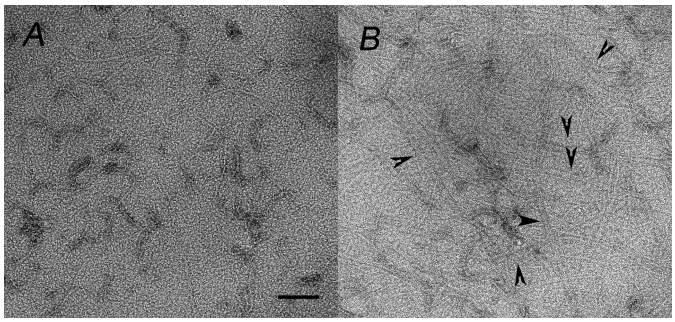

FIGURE 3. **Electron microscopy of FtsZ polymers.** Shown is FtsZ (6 μM) in working buffer with 100 mM KCl. Polymerization was triggered by adding either 1 mM GTP (*A*) or 0.4 mM GMPCPP (*B*). *Arrowheads* in *B* indicate the presence of some of the double filaments. *Scale bar* = 90 nm.

masses obtained were equivalent within error to those estimated from sedimentation and diffusion coefficients via the Svedberg equation (Table 1). The width of the $c(M)$ analysis represents the broadest possible M distribution, as the quality of the fit was comparable to the $c(s)$ analysis. As expected, the f/f_0 values obtained for the FtsZ polymers (Table 1) were much larger than those corresponding to compact spheres of identical masses (17).

Static light scattering profiles of GTP-FtsZ polymers with decreasing potassium acetate concentrations showed essentially the same decrease in intensity as with KCl buffers (Fig. 4). SV distributions, more complex than in KCl, showed the same trend (data not shown). This is in agreement with a previous study in which the equivalence of KCl and potassium acetate was determined through GTPase and kinetics measurements (8). Potassium acetate in magnesium-free buffers containing EDTA at neutral pH provokes the aggregation of GTP-FtsZ (data not shown), which otherwise exists as an unassembled species in KCl (5).

The Concerted Nature of the Transition between FtsZ Oligomers and Polymers Is Maintained at Lower K^+ Concentration—SV measurements previously conducted on FtsZ polymers at 500 mM KCl indicated the cooperative appearance of a narrow size distribution of finite oligomers with increasing concentrations of FtsZ (9) and magnesium (5). At 10–100 μM magnesium, an intermediate metastable species appears that rapidly evolves toward the high molecular weight species upon a slight increase in the cation content (5). Analysis of the concentration dependence of light scattering and diffusion coefficients further confirmed the cooperative appearance of a narrow distribution of high molecular weight species and allowed the mass of the polymers to be determined (5). To verify whether this concerted transition still described FtsZ polymerization at lower KCl concentration or if the polymerization process at different salt concentrations involved additional species other than a single assembled and unassembled FtsZ species, we conducted SV experiments at 100 mM KCl, varying the magnesium concentration within the 0–5 mM range. In the presence of EDTA, the sedimentation profile corresponded to that for monomers of FtsZ, as observed previously at 500 mM KCl (9). Sedimentation profiles at and below 100 μM magnesium showed a main slow sedimenting species accompanied by a minor fast species, the proportion of which increased at magnesium concentrations of 300 μM and above (Fig. 5). Profiles obtained at submillimolar and millimolar magnesium concentrations at this KCl concentration showed a content of assembled and unassembled proteins similar to those determined at 500 mM KCl. Fig. 5*A* depicts the fractional distribution of the slow (representing an ensemble of all unassembled material) and fast (representing, in turn, an ensemble of all assembled material) sedimenting species at 100 mM KCl with the magnesium content, calculated from these sedimentation profiles. Fractional distributions at 500 mM KCl, calculated from the SV data reported previously (5), are shown for comparison. The variation of slow and fast species with protein concentration at 100 mM KCl shows a very similar behavior to that at 500 mM KCl (Fig. 5*B*), calculated from the SV data reported previously (9). On the other hand, FCS experiments performed at 200 mM KCl showed that, as in 500 mM KCl (5), the diffusivity of assembled FtsZ remained independent of FtsZ concentration in the 10–37 μM range (Fig. 5*D*). Taken together, the SV and FCS data at variable Mg^{2+} and FtsZ concentrations, respectively, support the cooperative formation of a narrow distribution of preferred fibrils at KCl concentrations below 500 mM in the presence of GTP.

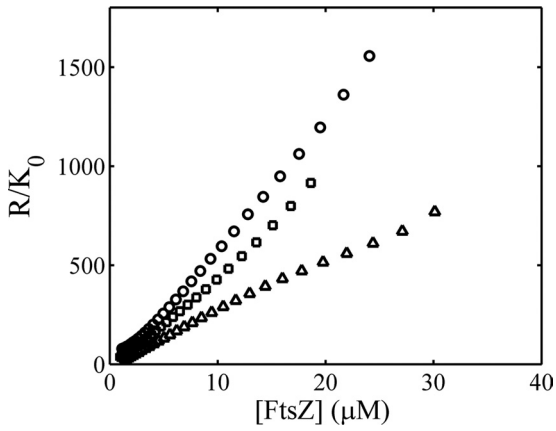

FIGURE 4. **Effect of potassium acetate on FtsZ assembly.** Shown is the concentration dependence of FtsZ scattering at 90° in the presence of GTP at 100 (*triangles*), 300 (*squares*), and 500 (*circles*) mM potassium acetate and 5 mM Mg^{2+}.

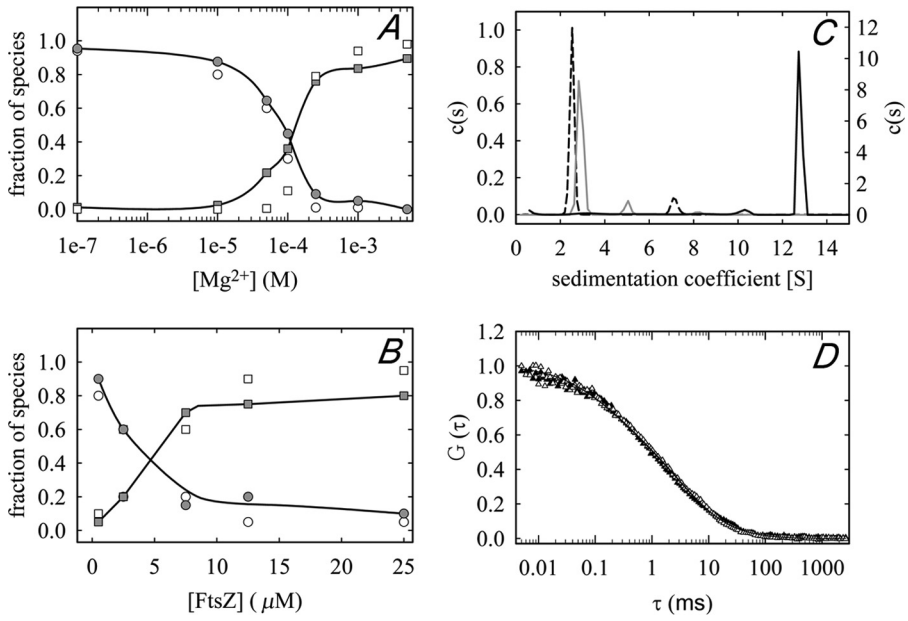

FIGURE 5. **FtsZ assembly at variable Mg^{2+} and protein concentrations.** *A* and *B*, fractional distributions of slow (2–5 S; *gray circles*) and fast (above 8.5 S; *gray squares*) sedimenting species depending upon the magnesium (12 μM FtsZ) and protein (5 mM magnesium) concentration, respectively, calculated from sedimentation profiles with 1 mM GTP in 100 mM KCl. *White symbols* correspond to the fractional distribution of the same species with 500 mM KCl, calculated from the sedimentation profiles reported previously (5, 9). *Lines* are meant only to guide the eye. For clarity, the metastable intermediate species found at 500 mM KCl with 10–100 μM magnesium (5) is not shown. *C*, representative sedimentation profiles of GTP-FtsZ in 100 mM KCl, from which the fractions in *A* and *B* were calculated, at the magnesium and protein concentrations specified. The *dashed line* (0.7 μM FtsZ and 5 mM Mg^{2+}) refers to the *y axis* on the *left*. The *grey line* (12 μM FtsZ and 10 μM Mg^{2+}) and the *black line* (12 μM FtsZ and 1 mM Mg^{2+}) refer to the *y axis* on the *right*. *D*, normalized FCS autocorrelation curves of 12 μM FtsZ (*white triangles*) and 37 μM FtsZ (*black triangles*) with 1 mM GTP at 200 mM KCl. The contribution of unassembled FtsZ was 15%. The concentration of Alexa Fluor 488-labeled FtsZ was 0.15 μM, and additional unlabeled FtsZ was added up to the final concentration.

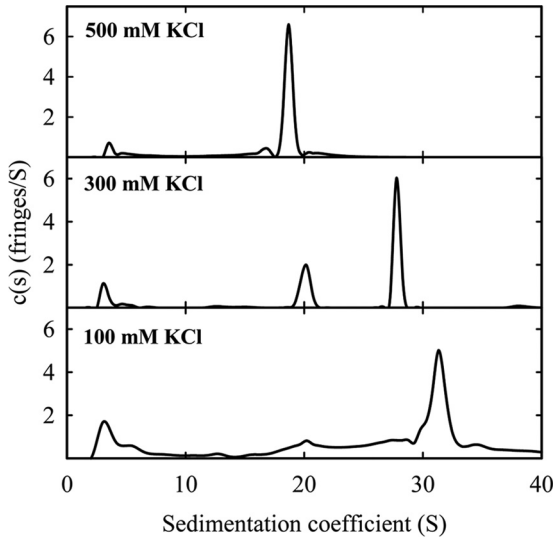

FIGURE 6. **Effect of KCl on GMPCPP-FtsZ sedimentation.** Shown are typical sedimentation coefficient distributions of FtsZ (25 μM) with 1 mM GMPCPP in working buffer with the specified KCl concentrations.

GMPCPP-FtsZ Polymers Become Apparently Larger and More Heterogeneous upon Lowering the KCl Concentration—The effect of KCl on GMPCPP-FtsZ polymer size was found to be, apparently, the opposite of that observed in the presence of GTP (Fig. 6). In contrast with the homogeneous distribution of GTP-FtsZ polymers within the whole KCl range, GMPCPP-FtsZ polymer solutions at 100 mM KCl were highly polydisperse and quantitatively described by main species with *s* values larger than 30 S, significantly higher than the 19 S that characterized the sedimentation of these polymers in 500 mM KCl (this work and Ref. 5).

The larger size and increasingly heterogeneous nature of GMPCPP-FtsZ polymers upon lowering the KCl concentration was further evidenced by their translational diffusive behavior determined by DLS and FCS (Fig. 2*D*). The faster sedimentation and slower diffusion observed is compatible with an increase in the average mass of the polymers (Table 1). Calculations of the mass of the GMPCPP-FtsZ polymers via the Svedberg Equation were in very good agreement with *c*(*M*) distributions (Table 1). The level of heterogeneity of the GMPCPP-FtsZ solutions at and below 200 mM KCl precluded accurate mass calculations and analysis of the FCS and DLS data, and the quality of the fits of the model involving a single polymer to the autocorrelation functions was much lower than at higher salt concentration. EM images obtained under equivalent experimental conditions revealed the presence of mixtures of long single-stranded filaments and double filaments at 100 mM KCl (Fig. 3), whereas mainly single-stranded filaments were observed at 500 mM KCl (see supplemental Fig. S2 in Ref. 21).

The GTPase Activity of FtsZ Polymers Is Not Affected by KCl Concentration—GTPase activity was tested in GTP- and GMPCPP-FtsZ polymers at the 20–500 mM KCl range (Fig. 7). The hydrolytic activity of GTP-FtsZ polymers progressively increased when the salt concentration was raised from 20 to 100 mM, the concentration above which it remained, within error, constant. As expected, the overall GTPase activity of FtsZ polymers in which assembly was triggered by GMPCPP, the slowly hydrolyzable analog of GTP (22), was significantly lower at the

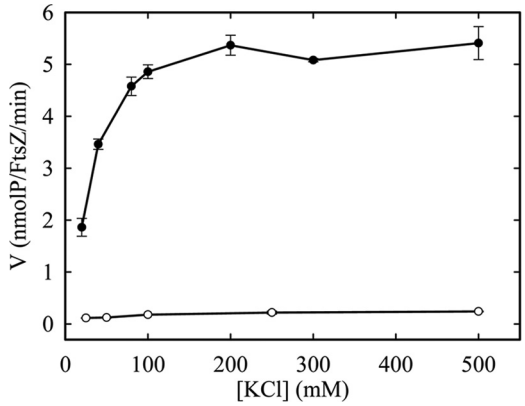

FIGURE 7. **Variation of the GTPase activity of GTP- and GMPCPP-FtsZ polymers with KCl content.** Shown are phosphate accumulation curves produced by GTP-FtsZ (*black circles*) and GMPCPP-FtsZ (*white circles*) polymers determined by the Malachite green method. The FtsZ concentration was 10 μM.

whole KCl range, whereas the change with salt concentration was negligible.

DISCUSSION

Using a variety of hydrodynamic and thermodynamic techniques, we have measured the effect of KCl on the size distribution and homogeneity of FtsZ species in the presence of GTP under steady-state conditions. Remarkably, the combined results presented here indicate that even when the final size of the GTP polymers becomes notably smaller upon lowering the KCl concentration, from ~85 (500 mM) to ~55 monomers (100 mM), several important features of the polymerization are maintained. The particular polymerization behavior consistently observed at high KCl leading to a narrow distribution of polymeric species (5, 9) is kept over the whole KCl range tested. Thus, with increasing protein and magnesium concentration, FtsZ undergoes a transition between a narrow distribution of low molecular weight species and a narrow size distribution of high molecular weight species. The insensitivity of the size of the fibrils to FtsZ concentration in the 10–37 μM range reported at 500 mM KCl is also a characteristic of FtsZ polymerization at 100 mM KCl, and variation of KCl concentration within this range has negligible influence on the critical concentration of assembly. Our results show the parallelism in the formation of those distributions of species at both salt extremes. The dependence of the fractions of species on increasing FtsZ concentration indicates a somehow softer transition until reaching the FtsZ concentration required for the formation of the polymer of definite size, in accordance with the polydispersity below 10 μM in the SV (9) and DLS (5) profiles. That transition is, however, sharper with increasing magnesium concentrations, as the polymeric species is already formed with micromolar cation content (5). Therefore, at neutral pH, this concerted transition is, in principle, generally applicable to GTP-induced FtsZ polymerization.

The observed reduction in size of GTP-FtsZ polymers at lower salt concentration is opposite the behavior of GDP-FtsZ oligomers, for which lowering the KCl concentration enhances Mg^{2+}-linked protein self-association (Fig. 2*A*) (12). Although the possible functional consequences of these findings are not yet known, they point toward different assembly pathways, which are mutually linked, for the formation of FtsZ oligomers (in the presence of GDP) and polymers (GTP-driven). Although the situation in the cell would be far more complex (as besides the presence of other cofactors and regulatory proteins affecting the filament, crowding and confinement could promote structures with different properties), fluctuations in salt content might favor a certain oligomer that could, in turn, favor a certain final polymeric species.

The similar behavior previously determined for GTP- and GMPCPP-FtsZ polymers with 500 mM KCl in terms of self-association, even rendering different final sizes of the polymers, was interpreted as a manifestation of a common association scheme (5, 21). The concentration dependence of scattering of FtsZ in GTP and GMPCPP was semiquantitatively well described by an equilibrium model assuming the self-assembly of FtsZ into linear fibrils that, above a certain size and because of the natural flexibility of FtsZ, tend to form cyclic structures involving the formation of side-to-side contacts between FtsZ monomers within the same filament (see Fig. 3 in Ref. 9). Our hydrodynamic measurements prove that this similarity is not maintained at lower salt concentrations, regrettably precluding a thorough parallel study to determine the possible effect of GTP hydrolysis and exchange under these lower salt conditions. The results obtained at the potassium range tested here in the presence of GTP clearly indicate that there must be an upper limit to steady-state fiber length for FtsZ assembly in GTP. Moreover, it has been recently shown that the inhibitory action of MinC, a regulator of FtsZ, also generates fibers with a narrow distribution of lengths (23). EM studies showed FtsZ polymers as mostly straight, mixed with curved filaments, what could be due to a smaller flexibility of the shorter filaments under these lower salt conditions (24, 25). It should be noted, however, that not only the size but also the composition might determine the flexibility of the fiber, as data of polymers in 100 μM magnesium and high salt, with sizes similar to those in lower salt, can be adequately described by the association scheme described above (21). The behavior of FtsZ in the presence of GMPCPP at low salt suggests that non-equilibrium reactions, such as GTP hydrolysis, GTP/GDP exchange, and fibril lateral interactions, may need to be taken into account to elaborate a more general description of FtsZ assembly. As explained in detail elsewhere (21), in the modeling exercise used to analyze FtsZ assembly at 500 mM potassium, non-equilibrium reactions were not taken into account, as they were not needed to get the *simplest* description that explains the combined experimental data.

The sizes of the polymers in 500 mM KCl reported here and previously by static light scattering (5) are in excellent agreement with those determined by atomic force microscopy, 103 ± 26 and 137 ± 32 subunits for GTP-FtsZ and GMPCPP-FtsZ polymers (11). The wide range of lengths reported in different EM studies reflects the sensitivity of the polymer size to solution conditions. At 50–100 mM salt, polymer size ranges between 50 (~196 nm) (25, 26) and 60 (~250 nm) (26) subunits in KCl and between 20 (~92 nm) (27, 28) and 40 (8, 28) subunits in acetate, falling in the range of ~55 units estimated here with 100 mM KCl. This distribution of sizes seems to be maintained

when using cryo-EM (see supplemental Table S1 in Ref. 26), which minimizes both the perturbations associated with sample preparation and the interactions with the underlying substrate. In agreement, our data suggest that KCl and KAc are exchangeable, as replacement of chloride by acetate has little effect on the assembly behavior of FtsZ in the presence of Mg^{2+}, as stated previously (2, 8, 14). Our estimates of sizes from solution measurements are then in good agreement with reported data from EM or atomic force microscopy under equivalent conditions and somehow reflect the variability in the features of the polymers within the intracellular K^+ concentration range (~0.1–1 M) (29). It is important to mention that, despite differences in the final polymer size depending on solution conditions, the narrow distribution of size is always maintained, as stated by biophysical methods and by EM (this work and Refs. 5, 9, 26, and 28). We may speculate that this particular feature of FtsZ, rendering species of uniform size, could determine important aspects of Z-ring assembly, as the frequency and distribution of interactions between filaments that could, in turn, be related to its functionality.

The KCl-dependent shift in polymer size observed here points toward an influence of K^+ concentration on the subunit turnover rate, considered to be the major determinant of FtsZ protofilament length (2, 8). GTPase activity is one of the main factors thought to determine the rate at which subunit exchange within the polymer takes place (30). However, our measurements indicate that the GTPase activity of FtsZ is saturated at 100 mM KCl and does not substantially vary within the KCl concentration range explored. Therefore, our observation that the filament size is smaller at lower salt concentration cannot be attributed to a change in the GTPase activity. This supports previous results showing a rather loose coupling between FtsZ polymerization and GTP hydrolysis (3). Hence, other factors would need to be invoked to explain the change in the subunit turnover rate. One possibility is related to a previously proposed dual-turnover mechanism based on the faster subunit exchange regarding GTP hydrolysis, where overall FtsZ turnover would result from that coupled to GTP hydrolysis and from the exchange of FtsZ-GTP subunits at the ends of the polymers (*i.e.* without nucleotide hydrolysis) (2, 8). In the absence of evidence pointing toward a hydrolysis localized at specific sites along the polymers, the fact that their narrow size distribution is maintained within the salt concentrations tested points toward K^+ affecting the second turnover mechanism. Another possibility is that the modulation of the size of FtsZ polymers may be related to binding of K^+ to very low affinity sites (7) different from the protein active center, which is already saturated at 100 mM KCl, favoring the elongation of the filaments.

Our results can help clarify how FtsZ fibers might be arranged to form the Z-ring, as its precise structure has not yet been solved, and the structural organization of FtsZ in the ring has therefore not been established. It has been proposed that this filament is composed of short subunits that somehow assemble to encircle the diameter of the bacteria (2). High resolution imaging has recently described the ring as a not uniform entity (31), which would fit with the expected plasticity of FtsZ fibers whose size and geometry can be modulated by slight changes in the microenvironment. Our data point in this direction, as we consistently found a narrow distribution of short filaments in the KCl physiological range, which, furthermore, was maintained under different experimental conditions and even in the presence of regulatory proteins (23, 32).

To conclude, we have shown here that the condensation-like behavior of FtsZ polymerization is a central feature of FtsZ assembly. The results presented here reinforce the idea that FtsZ assembles by forming a narrow size distribution of filaments with a turnover rate uncoupled from or loosely coupled to the GTP hydrolysis rate. These properties must be considered in more elaborated mechanistic models of protein assembly, as they are involved in the regulation of the biochemical activities leading to the formation of the FtsZ complexes active in bacterial division.

Acknowledgments—We thank J. R. Luque-Ortega (Analytical Ultracentrifugation Facility, Centro de Investigaciones Biológicas) for assistance with SV experiments and analysis, F. Escolar (EM Facility, Centro de Investigaciones Biológicas) for technical assistance in transmission EM sample preparation, C. A. Royer for a laser loan and helpful discussions, and N. Ropero for technical assistance.

REFERENCES

1. Mingorance, J., Rivas, G., Vélez, M., Gómez-Puertas, P., and Vicente, M. (2010) Strong FtsZ is with the force: mechanisms to constrict bacteria. *Trends Microbiol.* **18,** 348–356
2. Erickson, H. P., Anderson, D. E., and Osawa, M. (2010) FtsZ in bacterial cytokinesis: cytoskeleton and force generator all in one. *Microbiol. Mol. Biol. Rev.* **74,** 504–528
3. Mendieta, J., Rico, A. I., López-Viñas, E., Vicente, M., Mingorance, J., and Gómez-Puertas, P. (2009) Structural and functional model for ionic (K^+/Na^+) and pH dependence of GTPase activity and polymerization of FtsZ, the prokaryotic ortholog of tubulin. *J. Mol. Biol.* **390,** 17–25
4. Pacheco-Gómez, R., Roper, D. I., Dafforn, T. R., and Rodger, A. (2011) The pH dependence of polymerization and bundling by the essential bacterial cytoskeletal protein FtsZ. *PLoS ONE* **6,** e19369
5. Monterroso, B., Ahijado-Guzmán, R., Reija, B., Alfonso, C., Zorrilla, S., Minton, A. P., and Rivas, G. (2012) Mg^{2+}-linked self-assembly of FtsZ in the presence of GTP or a GTP analogue involves the concerted formation of a narrow size distribution of oligomeric species. *Biochemistry* **51,** 4541–4550
6. Mukherjee, A., and Lutkenhaus, J. (1999) Analysis of FtsZ assembly by light scattering and determination of the role of divalent metal cations. *J. Bacteriol.* **181,** 823–832
7. Tadros, M., González, J. M., Rivas, G., Vicente, M., and Mingorance, J. (2006) Activation of the *Escherichia coli* cell division protein FtsZ by a low-affinity interaction with monovalent cations. *FEBS Lett.* **580,** 4941–4946
8. Chen, Y., and Erickson, H. P. (2009) FtsZ filament dynamics at steady state: subunit exchange with and without nucleotide hydrolysis. *Biochemistry* **48,** 6664–6673
9. González, J. M., Vélez, M., Jiménez, M., Alfonso, C., Schuck, P., Mingorance, J., Vicente, M., Minton, A. P., and Rivas, G. (2005) Cooperative behavior of *Escherichia coli* cell-division protein FtsZ assembly involves the preferential cyclization of long single-stranded fibrils. *Proc. Natl. Acad. Sci. U.S.A.* **102,** 1895–1900
10. Small, E., and Addinall, S. G. (2003) Dynamic FtsZ polymerization is sensitive to the GTP to GDP ratio and can be maintained at steady state using a GTP-regeneration system. *Microbiology* **149,** 2235–2242
11. Mateos-Gil, P., Paez, A., Hörger, I., Rivas, G., Vicente, M., Tarazona, P., and Vélez, M. (2012) Depolymerization dynamics of individual filaments of bacterial cytoskeletal protein FtsZ. *Proc. Natl. Acad. Sci. U.S.A.* **109,**

8133–8138
12. Rivas, G., López, A., Mingorance, J., Ferrándiz, M. J., Zorrilla, S., Minton, A. P., Vicente, M., and Andreu, J. M. (2000) Magnesium-induced linear self-association of the FtsZ bacterial cell division protein monomer. The primary steps for FtsZ assembly. *J. Biol. Chem.* **275,** 11740–11749
13. Reija, B., Monterroso, B., Jiménez, M., Vicente, M., Rivas, G., and Zorrilla, S. (2011) Development of a homogeneous fluorescence anisotropy assay to monitor and measure FtsZ assembly in solution. *Anal. Biochem.* **418,** 89–96
14. González, J. M., Jiménez, M., Vélez, M., Mingorance, J., Andreu, J. M., Vicente, M., and Rivas, G. (2003) Essential cell division protein FtsZ assembles into one monomer-thick ribbons under conditions resembling the crowded intracellular environment. *J. Biol. Chem.* **278,** 37664–37671
15. Hoenig, M., Lee, R. J., and Ferguson, D. C. (1989) A microtiter plate assay for inorganic phosphate. *J. Biochem. Biophys. Methods* **19,** 249–251
16. Schuck, P. (2000) Size-distribution analysis of macromolecules by sedimentation velocity ultracentrifugation and Lamm equation modeling. *Biophys. J.* **78,** 1606–1619
17. Laue, T. M., Shah, B. D., Ridgeway, T. M., and Pelletier, S. L. (1992) Computer-aided interpretation of analytical sedimentation data for proteins. in *Analytical Ultracentrifugation in Biochemistry and Polymer Science* (Harding, S. E., Rowe, A. J., and Horton, J. C., eds) pp. 90–125, Royal Society of Chemistry, Cambridge, United Kingdom
18. Fernández, C., and Minton, A. P. (2008) Automated measurement of the static light scattering of macromolecular solutions over a broad range of concentrations. *Anal. Biochem.* **381,** 254–257
19. Svedberg, T., and Pedersen, K. O. (1940) *The Ultracentrifuge*, Clarendon Press, Oxford, United Kingdom
20. Monterroso, B., Alfonso, C., Zorrilla, S., and Rivas, G. (2013) Combined analytical ultracentrifugation, light scattering and fluorescence spectroscopy studies on the functional associations of the bacterial division FtsZ protein. *Methods* **59,** 349–362
21. Monterroso, B., Rivas, G., and Minton, A. P. (2012) An equilibrium model for the Mg^{2+}-linked self-assembly of FtsZ in the presence of GTP or a GTP analogue. *Biochemistry* **51,** 6108–6113
22. Salvarelli, E., Krupka, M., Rivas, G., Vicente, M., and Mingorance, J. (2011) Independence between GTPase active sites in the *Escherichia coli* cell division protein FtsZ. *FEBS Lett.* **585,** 3880–3883
23. Hernández-Rocamora, V. M., García-Montañés, C., Reija, B., Monterroso, B., Margolin, W., Alfonso, C., Zorrilla, S., and Rivas, G. (2013) MinC protein shortens FtsZ protofilaments by preferentially interacting with GDP-bound subunits. *J. Biol. Chem.* **288,** 24625–24635
24. Popp, D., Iwasa, M., Narita, A., Erickson, H. P., and Maéda, Y. (2009) FtsZ condensates: an *in vitro* electron microscopy study. *Biopolymers* **91,** 340–350
25. Huecas, S., Llorca, O., Boskovic, J., Martín-Benito, J., Valpuesta, J. M., and Andreu, J. M. (2008) Energetics and geometry of FtsZ polymers: nucleated self-assembly of single protofilaments. *Biophys. J.* **94,** 1796–1806
26. Turner, D. J., Portman, I., Dafforn, T. R., Rodger, A., Roper, D. I., Smith, C. J., and Turner, M. S. (2012) The mechanics of FtsZ fibers. *Biophys. J.* **102,** 731–738
27. Romberg, L., Simon, M., and Erickson, H. P. (2001) Polymerization of Ftsz, a bacterial homolog of tubulin. Is assembly cooperative? *J. Biol. Chem.* **276,** 11743–11753
28. Chen, Y., and Erickson, H. P. (2005) Rapid *in vitro* assembly dynamics and subunit turnover of FtsZ demonstrated by fluorescence resonance energy transfer. *J. Biol. Chem.* **280,** 22549–22554
29. Record, M. T., Jr., Courtenay, E. S., Cayley, S., and Guttman, H. J. (1998) Biophysical compensation mechanisms buffering *E. coli* protein-nucleic acid interactions against changing environments. *Trends Biochem. Sci.* **23,** 190–194
30. Romberg, L., and Mitchison, T. J. (2004) Rate-limiting guanosine 5′-triphosphate hydrolysis during nucleotide turnover by FtsZ, a prokaryotic tubulin homologue involved in bacterial cell division. *Biochemistry* **43,** 282–288
31. Strauss, M. P., Liew, A. T., Turnbull, L., Whitchurch, C. B., Monahan, L. G., and Harry, E. J. (2012) 3D-SIM super resolution microscopy reveals a bead-like arrangement for FtsZ and the division machinery: implications for triggering cytokinesis. *PLoS Biol.* **10,** e1001389
32. Hernández-Rocamora, V. M., Reija, B., García, C., Natale, P., Alfonso, C., Minton, A. P., Zorrilla, S., Rivas, G., and Vicente, M. (2012) Dynamic interaction of the *Escherichia coli* cell division ZipA and FtsZ proteins evidenced in nanodiscs. *J. Biol. Chem.* **287,** 30097–30104

Control by Potassium of the Size Distribution of *Escherichia coli* FtsZ Polymers Is Independent of GTPase Activity

Rubén Ahijado-Guzmán, Carlos Alfonso, Belén Reija, Estefanía Salvarelli, Jesús Mingorance, Silvia Zorrilla, Begoña Monterroso and Germán Rivas

J. Biol. Chem. 2013, 288:27358-27365.
doi: 10.1074/jbc.M113.482943 originally published online August 12, 2013
